



ELSEVIER

Journal of Alloys and Compounds 320 (2001) 320–325

Journal of
ALLOYS
AND COMPOUNDS

www.elsevier.com/locate/jallcom

Calorimetric study of maltitol: correlation between fragility and thermodynamic properties

N. Lebrun^{a,*}, J.C. van Miltenburg^b

^aLaboratoire de Dynamique et Structure des Matériaux Moléculaires (UPRESA 8024), Université des Sciences et Technologies de Lille, UFR de Physique, Bât. P5, 59655 Villeneuve d'Ascq Cedex, France

^bChemical Thermodynamics Group, Faculty of Chemistry, Utrecht University, Padualaan 8, 3584 CH Utrecht, The Netherlands

Abstract

The heat capacity of maltitol was measured with an adiabatic calorimeter. The crystalline form was measured from 100 to 425 K ($T_m = 420$ K), the glass form from 249 K to T_g (around 311 K) and the liquid form from T_g to 400 K. The heat of melting is 55.068 kJ mol⁻¹. The calorimetric glass transition occurs at about $T_g = 311$ K with a sudden jump of the heat capacity $\Delta C_p(T_g)$ of about 243.6 J mol⁻¹ K⁻¹. The excess entropy between the under-cooled liquid and the crystal was calculated from the heat capacity data and was used to estimate the Kauzmann temperature T_K , which was found to be 50 K below T_g . $\Delta C_p(T_g)$ and T_K values for maltitol were compared with those of other compounds such as sugars, polyols and hydrogen-bonded liquids. It was found that the glass former maltitol is a 'fragile' liquid from the thermodynamic point of view. © 2001 Elsevier Science B.V. All rights reserved.

Keywords: Glass transition; Calorimetry; Heat capacity; Entropy; Thermodynamic; Fragility

1. Introduction

When cooled without crystallisation below the melting temperature, an under-cooled liquid vitrifies at a temperature called the glass transition temperature, T_g . The rearrangement motions of the molecules that are present in the under-cooled liquid then become frozen-in on the time scale of the experiment below T_g . This induces a change in the thermodynamic behavior, which is characterised by a more or less pronounced drop in the heat capacity [1].

The relaxation time of molecular movements τ , which occurs in an under-cooled liquid, follows a non-Arrhenius temperature dependence, which is more or less pronounced depending on the substance. This has been attributed to resistance against the structural changes occurring in glass formers. A fragility index has been introduced to quantify this resistance. It is defined as the slope m measured at T_g of the relaxation curve in an Arrhenius plot [2]. Depending on the value of m , ranging from 16 (pure Arrhenius behaviour) to 200 (strong Vogel–Fulcher–Tamman behaviour [3,4]), glass formers are classified as being 'strong' or 'fragile' [5–7].

This dynamic definition of the fragility index was tentatively correlated to the thermodynamic characteristic of the calorimetric glass transition [8], which is observed to vary strongly from one type of glass former to another. Namely, the more fragile (i.e. the more non-Arrhenius) the glass is, the larger the ratio $C_{p,liq}/C_{p,crys}$ appears to be, where $C_{p,liq}$ and $C_{p,crys}$, respectively, are the heat capacities of the liquid and the crystal. Such thermodynamic behaviour can be related to the position of T_g with regard to the iso-entropic Kauzmann temperature T_K [9]. The latter is closer to T_g if the relative amplitude of the C_p jump is large and the departure from pure Arrhenius behaviour is significant. However, such a correlation is not without exceptions, nor yet clearly established. Indeed, some defects may additionally contribute to the heat capacity in the glass transition temperature range. For some molecular hydrogen-bonded glass formers, which are of intermediate fragility, the relative change in the heat capacity at T_g is even larger than for fragile liquids [8].

The purpose of the present study was to determine if this feature, assigned to hydrogen bond contributions [8], is commonly observed in molecular liquids with numerous hydrogen bonds. The heat capacity of maltitol (1,4-*O*- α -D-glucopyranosyl-D-glucitol) was measured precisely in all the condensed states (liquid, metastable liquid, solid and glass) with an adiabatic calorimeter. This carbohydrate

*Corresponding author. Tel.: +33-3-2043-6487; fax: +33-3-2043-4084.

E-mail address: nathalie.lebrun@univ-lille1.fr (N. Lebrun).

substance, which is widely used in low calorie and dietary foods [10–14], was chosen for this study because of its complex molecular structure with numerous hydrogen bonds [15]. The compound itself also offers a practical advantage for the investigation of glass former behavior as no interfering re-crystallisation effect is observed.

Some scarce thermodynamic data for maltitol were found in the literature, namely the temperature and enthalpy of melting [16–18], the glass transition temperature and the heat capacity jump at T_g were measured by Roos and Siniti [17,18]. Also, some investigations of the relaxation enthalpy processes in glass were carried out by Siniti [18]. However, precise thermodynamic heat capacity C_p data have not yet been determined for this compound.

The precise thermodynamic measurements which are presented in this paper allow us to determine the heat capacity jump at T_g and the temperature dependence of the configurational entropy. The ‘thermodynamic’ fragility of maltitol was deduced and compared with that of other glass formers. It is especially interesting to discuss this point by reference to other sugars and hydrogen-bonded glass formers.

2. Experimental

Commercial maltitol (1,4-*O*- α -D-glucopyranosyl-D-glucitol), the purity of which was stated to be 98%, was purchased from Aldrich and was dried before use.

The heat capacity of maltitol was measured in the temperature range between 100 and 425 K using a home-made adiabatic calorimeter described elsewhere [19].

The heat capacity measurement was carried out using a standard intermittent heating method, i.e. repetition of equilibration (from 600 to 1000 s) and heating intervals (808 s). During the heating period, the sample temperature is raised by an increment between 2 and 3 K. The heating period is followed by an equilibration period, in which the sample temperature is measured as a function of time. The first 1–2 min of this period are required for the sample cell to reach a uniform temperature distribution. Then the calorimetric temperature drift observed for the later part of the period reflects the combined effect from the small heat leakage due to the incomplete adiabaticity and from any enthalpy relaxation that the sample might show, such as melting, crystallisation and glass transition.

The heat capacity of the sample is given by

$$C_p = \frac{Q + q_{\text{exch}}}{T}$$

where $q_{\text{exch}} = C(dT/dt)$. ΔT is the temperature increase caused by supplying a known quantity of electric energy Q during the energising period. In most heat capacity measurements, Q is of the order of 30 J. ΔT is calculated using extrapolation of the temperature time curve recorded in the second half of the equilibration period before and after the

energising period to the mid-point of the heating period. C is the total heat capacity of the system sample vessel. dT/dt is the temperature drift calculated for the second half of the equilibration period by a linear fit of the temperature time curves. Deviations of temperature drifts (0.5 – $1 \mu\text{K s}^{-1}$) are usually found in an empty vessel experiment or in a temperature region where the compound is in thermodynamic equilibrium (no exo- or endo-thermal effect). The regions where no relaxation processes take place are used to make a polynomial fit of the heat exchange with the surroundings. This fit is then applied to the part of the measurement where relaxation effects occur. The precision of the heat capacity measurement is on the order of 0.02% or better (depending also on the amount of compound).

The quantity of sample loaded in the calorimeter vessel was 3.96678 g (0.01152 mol). Helium gas (1000 Pa) was charged into the dead space of the sample vessel to enhance the thermal equilibrium between the sample and the vessel. The calorimeter vessel was closed with an annealed gold gasket and mounted in an evacuated space surrounded by two temperature-regulated shields within the cryostat. The temperatures of the inner adiabatic shield and the wire heater body were kept as close as possible to the temperature of the vessel. A calibrated platinum thermometer within the vessel enabled measurement of the temperature of the sample, leading to a precision of about 0.0002 K. The cryostat was filled with liquid nitrogen. A few millimetres of dry helium were admitted into the system in order to obtain a short cooling time, and were pumped out before the measurement was started.

3. Results and discussion

3.1. Heat capacity and enthalpy data

Since, once melted, the under-cooled liquid does not crystallise, the heat capacity of the crystalline sample was first measured between 100 and 425 K with an average rate of 0.128 K min^{-1} . The molten sample was then re-cooled from 425 to 249 K at about 4.3 K min^{-1} . The heat capacities of the glassy state and the metastable liquid were determined on re-heating from 249 to 400 K at about 0.068 K min^{-1} . To access high temperature measurements, the liquid nitrogen was removed. The sample–vessel system was then maintained for 12 h at 320 K. Owing to the fact that the life-time of the metastable liquid is long, the heat capacity was measured precisely in all the metastable domains by the intrinsically slow adiabatic calorimetry technique.

The molar heat capacity data for the liquid, crystal and glass are listed in Table 1. Figs. 1 and 2 reproduce graphically the evolution of the heat capacity and the corresponding enthalpy increment with temperature for all condensed states.

Table 1

Experimental molar heat capacities of maltitol, C_{pm} ($M = 344.316 \text{ g mol}^{-1}$, $R = 8.31451 \text{ J mol}^{-1} \text{ K}^{-1}$)

T/K	C_{pm}/R	T/K	C_{pm}/R	T/K	C_{pm}/R	T/K	C_{pm}/R
Series 1	Crystal	280.5058	406.97			347.9148	786.59
		283.4640	411.60	Melting		349.9021	788.45
		286.0411	414.20				351.8905
103.5829	159.32	288.3393	420.23	420.1883	27085.74	353.8791	792.44
107.5799	165.55	290.9766	423.85	420.3144	21754.94	355.8643	795.15
111.4841	171.45	293.9433	428.33	421.2069	2091.11	357.8500	797.86
115.2809	176.98	296.9084	432.77	422.8278	856.94	359.8363	799.76
118.9845	182.35	299.8779	436.74			361.8236	801.91
122.6096	187.81	302.8459	441.01	Series 2	Glass	363.8121	804.09
126.1648	193.10	305.8120	445.72				
129.6560	198.10	308.7767	450.22	251.7888	347.61	367.7911	808.43
133.0895	202.86	311.7393	454.97	254.2192	395.27	369.7785	810.34
136.4692	207.78	314.6994	459.60	256.6041	399.68	371.7666	812.26
139.8003	212.41	317.6628	464.38	258.9781	404.10	373.7559	814.51
143.0849	217.07	320.6299	469.01	261.3408	408.08	375.7460	816.45
146.3255	221.44	323.5948	473.29	263.6920	412.42	377.7374	818.45
149.5255	225.77	326.5576	478.07	266.0320	416.47	379.7265	820.67
152.6881	230.28	329.5184	483.38	268.3610	420.55	381.7167	822.70
155.8159	234.87	332.4770	488.16	270.6789	424.90	383.7091	824.60
158.9043	239.79	335.4388	493.05	272.9863	429.23	385.7034	826.68
161.9550	243.54	338.4039	497.99	275.2830	433.39	387.6984	828.74
164.9760	247.05	341.3671	502.97	277.5689	437.36	389.6914	830.55
167.9674	250.93	344.3298	507.63	279.8443	441.39	391.6866	832.45
170.9383	254.91	347.2918	512.18	282.1106	445.79	393.6835	834.05
173.8961	258.96	350.2534	516.66	284.3677	449.36	395.6782	836.35
176.8511	262.95	353.2194	521.32	286.6153	452.77	397.6747	838.03
179.8078	266.95	356.1886	526.12	288.8545	456.37	399.6733	840.10
182.7665	270.94	359.1566	531.35	291.0852	459.86		
185.7284	274.97	362.1224	536.42	293.3075	463.25		
188.6937	278.97	365.0858	541.49	295.5220	466.71		
191.6572	282.66	368.0527	547.09	297.7283	470.24		
194.6187	286.80	371.0229	552.32	299.9261	473.79		
197.5850	290.74	373.9908	557.94	302.1152	478.54		
200.5488	294.79	376.9566	563.52	304.2922	486.06		
203.5111	298.01	379.9242	570.13	306.4501	499.33		
206.4736	302.81	382.8938	577.07	308.5777	526.54		
209.4354	306.75	385.8594	584.92	310.6416	585.83		
212.3936	310.75	388.8228	593.17				
215.3582	314.83	391.7817	602.92	Undercooled	liquid		
218.3198	318.92	394.7329	615.48				
221.2818	322.90	397.6743	633.78	312.5849	697.51		
224.2450	326.97	400.5905	662.32	314.4070	773.64		
227.2096	331.02	403.4572	713.04	316.2289	752.09		
230.1751	335.09	406.2268	805.36	318.1478	750.62		
233.1359	339.22	408.8339	973.97	320.1255	753.08		
236.0969	343.29	411.2077	1267.32	322.1123	755.20		
239.0596	347.46	413.2514	1747.57	324.0991	757.80		
242.0178	351.65	414.8884	2520.11	326.0825	759.98		
244.9778	355.59	416.1333	3659.63	328.0661	762.44		
247.9399	360.03	417.0746	5018.66	330.0495	764.97		
250.8982	364.32	417.8057	6599.17	332.0336	767.28		
253.8608	367.66	418.3862	8434.59	334.0179	769.60		
256.8271	371.51	418.8533	10645.64	336.0016	771.98		
259.7913	375.87	419.2157	14752.96	337.9858	774.47		
262.7508	380.15	419.5036	17045.23	339.9709	776.90		
265.7066	384.52	419.7454	21402.59	341.9565	779.20		
268.6653	388.57	419.9409	26506.39	343.9421	781.80		
271.6261	393.35	420.0753	22318.33	345.9282	784.21		
274.5861	397.13						
277.5443	402.24						

The sharp heat capacity peak with a maximum at 420 K is due to the first-order solid–liquid phase transition, which is characterised by an extended region of excess heat capacities on the low temperature side. This was associated with a rapid increase of the enthalpy at the melting temperature, 420 K. By integrating the second-order polynomial fit of the heat capacities of the liquid and the

crystal (see Table 2), the enthalpy difference between the liquid and the crystal at the melting point ($T_m = 420 \text{ K}$) was calculated to be $\Delta H_m = 55.068 \text{ kJ mol}^{-1}$. The values of T_m and ΔH_m almost agree with previous data: 420 K and 56.43 kJ mol^{-1} [15], 413 K and 51.647 kJ mol^{-1} [16], 422 K and 50.614 kJ mol^{-1} [17], and 418 K and 60.496 kJ mol^{-1} [18].

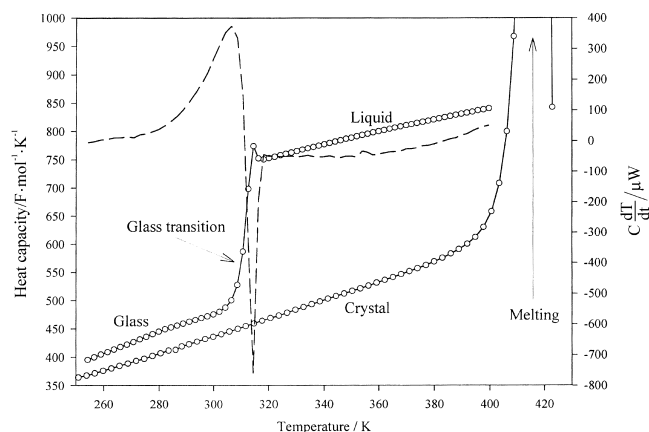


Fig. 1. Experimental molar heat capacities of maltitol for the different condensed states (liquid, crystal, glass). The C_p jump indicates the glass transition temperature $T_g = 311$ K ($\Delta C_p = 243.6$ J mol $^{-1}$ K $^{-1}$). The dashed curve is the variation of the drift with temperature in the glass transition domain.

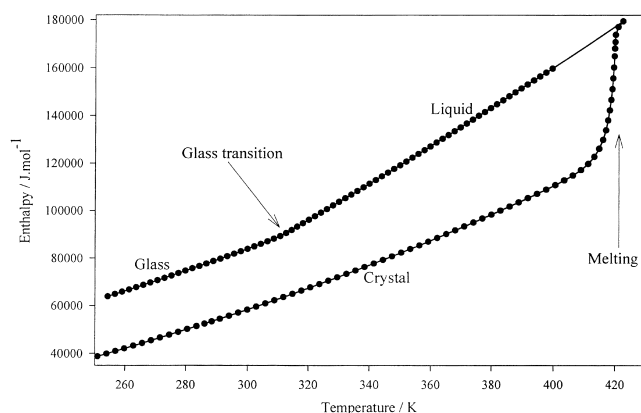


Fig. 2. Enthalpy curves for the different condensed states (liquid, glass and crystal). Crystal melting is observed at $T_m = 420$ K; the enthalpy of melting is 55.068 kJ mol $^{-1}$.

A sudden heat capacity jump ΔC_p was observed at 311 K and was estimated to be 243.6 J mol $^{-1}$ K $^{-1}$. Fig. 1 (dashed curve) also shows the rate of spontaneous temperature drift $C(dT/dt)$ around the glass transition. A large exothermic temperature drift starts to appear around 275 K, and becomes endothermic above 311 K. The sample-vessel system returns to normal behaviour at around 318 K. This behaviour of the temperature drift is a distinctive feature of the glass-liquid transition. This was associated with a change of the enthalpy slope, leading to an

Table 2

Coefficients of polynomial fits of the heat capacity for the different phases and the appropriate temperature ranges ($A_0 + A_1T + A_2T^2$ in J mol $^{-1}$ K $^{-1}$)

Phase and temperature range	A_0	A_1	A_2
Glassy state 251–270 K	-62.47428	1.80079	0
Liquid phase 320–422 K	133.24411	2.60606	-0.00209
Crystalline phase 103–370 K	45.13473	1.08629	0.00075

unfreezing of some rearrangement motion of the molecules. The glassy state transforms into an under-cooled liquid, the thermodynamic characteristics of which are very similar to those of the liquid since the slopes of the heat capacity curves are identical. This implies that the 'structures' of these two liquids are similar. No crystallisation took place on heating after the glass transition.

For the entire temperature range studied, the heat capacity of the glass is abnormally higher than that of the crystal (see Fig. 1). At 285 K, the difference between the heat capacity of the glass and the crystal was estimated to be 9.2% of the total heat capacity. In general, it amounts to about 2% [20]. This excess heat capacity is expected to reflect only the contribution of vibrational degrees of freedom. The observed unusually large contribution leads us to suspect that a secondary relaxation occurs below the glass transition [21], but is not observed here.

3.2. Calorimetric fragility and configurational entropy

The change in heat capacity observed at T_g is a useful indicator of fragility. In the 'strong' to 'fragile' classification scheme proposed by Angell [6,7], a 'strong' liquid exhibits very weak increases in heat capacity at T_g accompanied by Arrhenius behaviour of the dynamical relaxation process. 'Fragile' liquids show a large thermal manifestation at the glass transition temperature and non-Arrhenius behavior of the dynamic relaxation. The C_p value of the liquid, $C_{p,liq}$, relative to that of the crystal, $C_{p,crys}$, is shown as a function of T relative to T_g for maltitol in Fig. 3. The heat capacities were extrapolated using a second-order polynomial function with the calculated coefficients reported in Table 2. $C_{p,liq}/C_{p,crys}$ has a maximum of about 1.6 at T_g . This relatively high value indicates that maltitol has a high degree of fragility, as other sugars such as sucrose and glucose, as shown in Fig. 4.

Nevertheless, certain hydrogen-bonded liquids provide

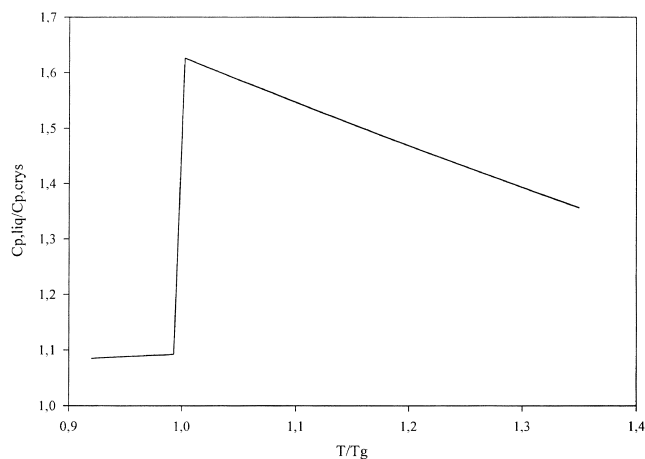


Fig. 3. Relative amplitude $C_{p,liq}/C_{p,crys}$ versus the normalised temperature T/T_g for maltitol.

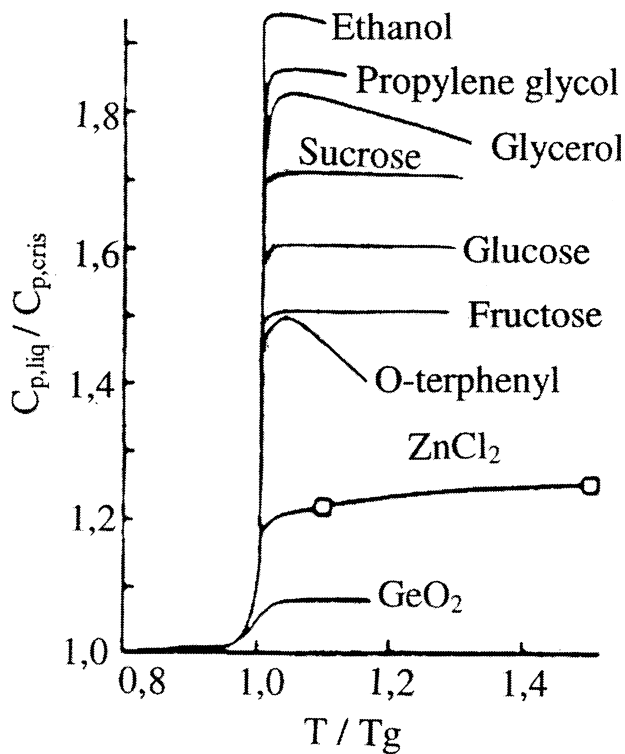


Fig. 4. Relative amplitude of $C_{p,\text{liq}}/C_{p,\text{crys}}$ versus the normalised temperature T/T_g for characteristic glass formers [7,8].

exceptions to this general pattern. For example, glycerol occupies an intermediate position in the classification for dynamic behaviour [22] and still exhibits a large change in heat capacity at its glass transition, i.e. a large value of the ratio $C_{p,\text{liq}}/C_{p,\text{crys}}$ as shown in Fig. 4. It has been suggested that such anomalous behaviour could be attributed to an additional Schottky-like contribution to the heat capacity. It would find its origin in the breaking of the hydrogen bonds. According to the strength of the hydrogen bonds, such a contribution would be able to give rise to an artificially large heat capacity jump. For example, in the case of *meta*-cresol, this component almost vanishes before T_g is reached, while, for fluorophenol, some hydrogen bonds still remain broken when the glass transition is reached [8]; another example of this behavior can be found for glycerol [23]. This hydrogen-breaking contribution to the heat capacity jump was quantified and located with temperature using a ‘bond on–bond off’ model [24]. Since maltitol is a hydrogen-bonded liquid, it is quite legitimate to consider the possible contribution of breaking hydrogen bonds leading to an anomalously high value of the $C_{p,\text{liq}}/C_{p,\text{crys}}$ ratio.

In order to eliminate this Schottky contribution, the thermodynamic fragility was determined from the isentropic Kauzmann temperature, T_K [9]. It has been shown that, with decreasing temperature, a large jump in the heat capacity at the glass transition is correlated to a more rapid decrease of the configurational entropy of the under-cooled liquid compared to the equilibrium crystal. Then the

entropy of the two condensed states, under-cooled liquid and crystal, become equal at the positive temperature T_K . T_K is lower than T_g and is closer to T_g for glass formers which exhibit a large heat capacity jump. T_K cannot be reached experimentally and is obtained from an evaluation of the excess entropy $\Delta S_{\text{excess}}(T)$ of the liquid over the crystal, defined as

$$S_{\text{excess}}(T) = S_{\text{liq}}(T) - S_{\text{crys}}(T) \\ = \Delta S_m - \int_T^{T_m} \frac{C_{p,\text{liq}}(T') - C_{p,\text{crys}}(T')}{T'} dT'$$

where ΔS_m is the entropy of melting, in this case $\Delta S_m = \Delta H_m/T_m = 131.1 \text{ J mol}^{-1} \text{ K}^{-1}$; S_{liq} and S_{crys} are the entropies of the liquid and crystal states, respectively.

Fig. 5 shows the temperature dependence of the excess entropy of maltitol deduced from the heat capacities of both the liquid and crystalline states extrapolated as a second-order polynomial function (see Table 2 for the coefficients). S_{excess} becomes nearly constant below T_g due to the freezing of the structure. From this plot, T_K was determined as $260.1 \pm 0.3 \text{ K}$. The uncertainty estimate is based on the accuracy of the extrapolation of the liquid heat capacity curve down to the temperature range of T_K . This temperature is not far from T_g (50 K below), as commonly observed for most ‘fragile’ liquids. Moreover, for ‘strong’ liquids, T_K is almost indistinguishable from 0 K.

In order to demonstrate the fragility of maltitol, it is interesting to compare the position of T_K relative to T_g with other glass formers. The value of $(T_g - T_K)/T_g$ for maltitol is weak compared to that for glycerol (see Table 3). It is concluded that the degree of ‘thermodynamic’ fragility is higher in maltitol than in glycerol. Since the heat capacity jump is larger in glycerol than in maltitol, the presence of hydrogen bonding in maltitol contributes less than in glycerol to the amplitude of the heat capacity jump.

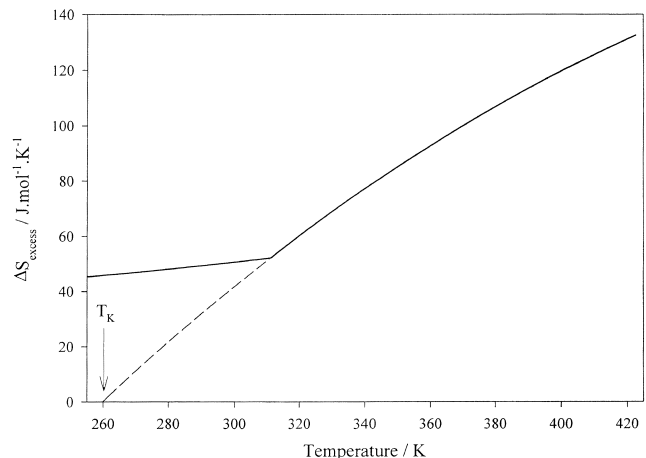


Fig. 5. Temperature evolution of the excess entropy of maltitol. The excess of liquid over solid entropy tends to vanish at 260 K.

Table 3

Fragility parameters of the dynamical relaxation process determined at T_g from 'fragile' to 'strong' liquids

'Fragile' to 'strong' liquids	T_g (K)	T_K (K)	$(T_g - T_K)/T_g$
Ethanol [26]	95	71	0.253
Propylene glycol [20]	167	^a	
Glycerol [27]	180	135	0.250
<i>O</i> -Terphenyl [20,28]	241	193	0.199
Maltitol (this study)	311	260	0.164

^a Not determined because of inability to crystallize.

4. Concluding remarks

The thermodynamic properties, heat capacity and entropy of maltitol were determined precisely using an adiabatic calorimeter.

The large value of the heat capacity jump at T_g and the relatively small difference between T_g (311 K) and T_K (260 K) leads to the conclusion, from a thermodynamic point of view, that the hydrogen-bonded liquid maltitol is a 'fragile' glass former. Its fragility is similar to that observed for some sugars and polyols. Since T_K is closer to T_g for maltitol than for glycerol, the presence of the hydrogen bonds in maltitol contributes less than in glycerol. This high thermodynamic fragility was confirmed by dynamical studies showing a large value of the dynamical fragility parameter m [25].

References

- [1] M.D. Ediger, C.A. Angell, S.R. Nagel, *J. Phys. Chem.* 100 (1996) 13200.

- [2] R. Bohmer, K.L. Ngai, C.A. Angell, D.J. Plazek, *J. Chem. Phys.* 99 (5) (1993) 4201.
- [3] H. Vogel, *Phys. Z.* 22 (1921) 645.
- [4] G.S. Fulcher, *J. Am. Ceram. Soc.* 8 (1923) 339.
- [5] C.A. Angell, in: K. Ngai, G.B. Wright (Eds.), *Relaxations in Complex Systems*, National Technical Information Service, U.S. Department of Commerce, Springfield, 1985.
- [6] C.A. Angell, *J. Phys. Chem. Solids* 49 (8) (1988) 863.
- [7] C.A. Angell, *J. Non-Cryst. Solids* 1 (1991) 131.
- [8] C.A. Angell, C. Alba-Simionesco, J. Fan, J.L. Green, Hydrogen bonding and the fragility of supercooled liquids and biopolymers, in: M.C. Bellissent-Funel, J. Dore (Eds.), *Hydrogen Bond Networks*, Kluwer Academic, 1994, p. 3.
- [9] W. Kauzmann, *Chem. Rev.* 43 (1948) 219.
- [10] F. Naito, *New Food Ind.* 13 (1971) 65.
- [11] S. Yoshizawa, S. Moriuchi, N. Hosoya, *J. Nutr. Sci. Vitaminol.* 21 (1975) 31.
- [12] P. Pittet, K. Acheson, K. Raman, E. Jequier, *Experientia* 31 (1975) 713.
- [13] A. Dahlqvist, U. Telenius, *Acta Physiol. Scand.* 63 (1965) 156.
- [14] J. Rundegren, T. Koulourides, T. Ericson, *Caries Res.* 14 (1980) 67.
- [15] S. Ohno, M. Hirao, *Carbohydr. Res.* 3 (1982) 163.
- [16] A. Raemy, T.F. Schweizer, *J. Thermal Anal.* 28 (1983) 95.
- [17] Y. Roos, *Carbohydr. Res.* 238 (1993) 39.
- [18] M. Siniti, Thesis No. 95ISAL0041, INSA, Lyon, 1995.
- [19] J.C. van Miltenburg, G.J.K. van der Berg, M.J. van Bommel, *J. Chem. Thermodyn.* 19 (1987) 1129.
- [20] S.S. Chang, A.B. Bestul, *J. Chem. Phys.* 56 (1972) 503.
- [21] J. Jäckle, *Rep. Prog. Phys.* 49 (1986) 171.
- [22] N. Menson, K.P. O'Brien, P.K. Dixon, L. Wu, S.R. Nagel, B.D. Williams, J.P. Carini, *J. Non-Cryst. Solids* 141 (1992) 61.
- [23] A. Barkatt, C.A. Angell, *J. Chem. Phys.* 70 (1979) 901.
- [24] C.A. Angell, *J. Phys. Chem.* 75 (1971) 3698.
- [25] A. Faivre, L. David, J. Perez, *J. Phys. II* (1997) 1635.
- [26] O. Haida, H.G. Suga, S. Seki, *J. Chem. Thermodyn.* 9 (1977) 113.
- [27] C.A. Angell, K.J. Rao, *J. Chem. Phys.* 57 (1972) 470.
- [28] P.K. Dixon, S.R. Nagel, *Phys. Rev. Lett.* 61 (1988) 341.